Food Research International 160 (2022) 111716

Contents lists available at ScienceDirect

Food Research International

journal homepage: www.elsevier.com/locate/foodres

Understanding the early-stage release of volatile organic compounds from rapeseed oil during deep-frying of tubers by targeted and omics-inspired approaches using PTR-MS and gas chromatography

Tomasz Majchrzak *, Mariusz Marć, Andrzej Wasik

Department of Analytical Chemistry, Faculty of Chemistry, Gdansk University of Technology, Gdansk, Poland

ARTICLE INFO

Keywords:
Food
Frying
VOCs
Real-time analysis
PTR-MS
Gas chromatography
SPME
Molecular networks

ABSTRACT

During deep-frying, a plethora of volatile products is emitted with the fumes. These compounds could act as oil quality indicators and change the indoor air composition leading to health risks for occupants. The presented experiments focus on deep-frying of different tubers in rapeseed oil at different frying temperatures. Here, two scenarios for real-time monitoring of volatile organic compounds (VOCs) using proton transfer reaction mass spectrometry (PTR-MS) were proposed. The first, targeted, involved the application of gas chromatography with a flame ionization detector (GC-FID). The second, omics-inspired, involved the use of solid-phase microextraction (SPME) along with gas chromatography-mass spectrometry (GC-MS) and molecular networking algorithm as a complementary tool to the PTR-MS analysis. In a targeted approach, it was shown that the emission profile of pentanal and hexanal depends on the frying temperature and as the temperature increases, a sudden release of these compounds can be observed in the first minutes of frying. Meanwhile, using an omics-inspired protocol enables finding the relation between 1,4-heptadienal and 2-heptanone, octanal and limonene emissions. Using both approaches it was possible to record real-time changes in emission profiles of various oils' degradation products. It was also observed that the emission profiles of VOCs are strictly related to the frying temperature and the type of fried tuber.

1. Introduction

Tracking the changes that occur during food processing is an integral part of food analysis. Compositional changes in thermally processed foods can enhance flavour, increase product digestibility, or modify product texture. On the other hand, it can lead to the formation of harmful chemical compounds, which can then be consumed or inhaled by consumers during food preparation (Bordin, Kunitake, Aracava, & Trindade, 2013; Hosseini, Ghorbani, Meshginfar, & Mahoonak, 2016; Zhang, Saleh, Chen, & Shen, 2012). Particular attention should be paid to the frying process, in which the transformations occurring both in food and in oil should be considered simultaneously. The products of thermal degradation of oil can migrate deep into the food (Bouchon, 2009) or can be emitted along with frying fumes. The analysis of the generated fumes may indirectly contribute to the assessment of oil quality.

For almost 40 years, there is a good understanding of the type and amount of compounds emitted during frying (Frankel, 1983). Some of them, for example, unsaturated or saturated aldehydes, products of fatty acid oxidation, can indicate the degree of thermal decomposition of oil and can be related to the characteristic unpleasant off-flavour (Katragadda, Fullana, Sidhu, & Carbonell-Barrachina, 2010). They may also pose a significant risk of lung inflammation, including carcinogenicity (Arı, Ertürk Arı, Yenïsoy-Karakaş, & Gaga, 2020; Lu et al., 2021). Moreover, frying compounds such as acrolein (Stevens & Maier, 2008), acrylamide (Mogol & Gökmen, 2016), polycyclic aromatic hydrocarbons (PAHs) (Yao et al., 2015), BTEX, and secondary organic aerosols (SOA) (Atamaleki, Motesaddi Zarandi, Massoudinejad, Esrafili, & Mousavi Khaneghah, 2022) may pose serious health risks.

The exact emission characteristics of these compounds in frying fumes were unknown until recently, mainly due to equipment limitations, which prevented effective analysis in real-time. Commonly used techniques, mostly based on gas chromatography (GC), require sample collection before analysis, which causes difficulties in capturing short-term transformations occurring, for instance, in the first seconds of frying. The solution may be the application of direct injection mass

* Corresponding author.
E-mail address: tomasz.majchrzak@pg.edu.pl (T. Majchrzak).

https://doi.org/10.1016/j.foodres.2022.111716
Received 2 April 2022; Received in revised form 6 July 2022; Accepted 19 July 2022
Available online 22 July 2022

spectrometry techniques (DI-MS), of which proton transfer reaction mass spectrometry (PTR-MS) is gaining popularity (Majchrzak et al., 2021a, 2021b).

The introduction of PTR-MS in the mid-90s of the 20th century (Hansel et al., 1995) has changed the perception of processes occurring in the environment (Hewitt, Hayward, & Tani, 2003), the human body (Zhan, Duan, & Duan, 2013), and in foods (Biasioli, Gasperi, Yeretzian, & Märk, 2011). In brief, the technique uses chemical ionization through proton transfer (usually with H_3O^+ as a proton donor) to 'softly' ionize trace-level volatiles found in the air (Ellis & Mayhew, 2014). It is remarkably successful in tracking emissions from foodstuffs, whether during processing or by examining aroma release during consumption (Majchrzak et al., 2021a, 2021b). There are known examples of using this technique to monitor cooking (Dimitri et al., 2013), coffee roasting (Gloess et al., 2014) and brewing process (López, Wellinger, Gloess, Zimmermann, & Yeretzian, 2016), baking (Pico, Khomenko, Capozzi, Navarini, & Biasioli, 2020), and frying (Majchrzak & Wasik, 2021). In the case of frying, the vast majority of research covers tracing volatiles during a long-lasting frying process, focusing mostly on its impact on indoor air quality (Arata et al., 2021; Majchrzak et al., 2021a, 2021b). Studies focusing on early-stage emission are still lacking. This, in turn, can be valuable information in determining exposure to VOCs during frying. In addition, understanding how volatile aroma compounds are generated can be applied to the design of palatable foods.

However, the application of PTR-MS involves a trade-off between real-time analysis and efficient identification of chemical structures. The main limitation is discrimination between isomers (Majchrzak, Wojnowski, Rutkowska, & Wasik, 2020). In addition, the resolution is an important factor - if insufficient, it may seriously hinder the identification of isobaric compounds. To solve this, GC can be used to support and complement the PTR-MS analysis (Majchrzak et al., 2018). This parallel use of GC and PTR-MS enables the efficient identification of compounds while maintaining real-time measurements using PTR-MS.

Using GC, the two approaches can be considered. The first, so-called targeted analysis, is when the GC is used to determine and PTR-MS for monitoring of the known compounds in frying fumes. GC is used to characterize, as comprehensively as possible, the volatile profile and identify its unknown components. Further interpretation of the obtained results can be challenging, hence the need for appropriate data analysis tools. In metabolomics, lipidomics, proteomics or other omics pipelines, this is referred to as bioinformatics (Schneider & Orchard, 2011). Recently in bioinformatics, the concept of molecular networking (MN) has been gaining popularity, since this strategy enables the interpretation of complex datasets, such as high-resolution LC or GC data (Aksenov et al., 2021; Vincenti et al., 2020). Briefly, the MN contains nodes and edges, representing detected features and similarities between them, respectively. The more similar the signals are, the stronger the cosine similarity (CS) between them is, thus nodes of such singnals are located closer in MN. Then, the pairs of nodes are connected according to the CS and the more complex connections are formed.

This study aimed to identify and monitor VOCs in emitted fumes during the deep-frying of different tubers in rapeseed oil. For this purpose, two approaches were proposed, the first targeted and the second omics-inspired. In the first approach, the PTR-MS real-time monitoring was supported by GC-FID. In the second, the MN based on GC-MS data was performed and then selected volatiles were monitored using PTR-MS. Additionally, the differences between various frying temperatures and fried tubers were addressed.

2. Materials and methods

2.1. Materials

The potato (*Solanum tuberosum)* tubers of *Gala,* all-purpose, AB-type and thermotolerant potatoes as well as sweet potatoes (*Ipomoea batatas)* were purchased in the local markets in Gdansk, Poland. The C-type potatoes *Innovator*, commercially used for the production of fries, were purchased from online distribution. The tubers were cut into a regular cube with 1.5 ± 0.2 cm side and a weight of 5.0 ± 0.1 g. The potato cubes were fried for 10 min. After frying their weight decreased to 2.5 ± 0.2 g. The visual evaluation proved that when fried at 180 °C, the potato cube was ready to eat after about 5 min, while after 10 min it showed a significant degree of blackening (See Figure S1, Supplementary Materials). The water content of tubers of *Gala*, *Innovator* and sweet potato before frying were 76.2 ± 2.6%, 66.5 ± 4.7% and 75.2 ± 2.9%, respectively (assessed based on loss on drying method). Bottles of rapeseed oil used for frying came from the same batch and the same manufacturer and were stored in a dark and cold place before the experiment. The quality of oil before, during and after frying was assessed by measuring the peroxide value (PV), total polar material (TPM) and thermal stability based on the Rancimat method (see Table S1 and Table S2, Supplementary Materials). Both pentanal (CAS: 110-62-3) and hexanal (CAS: 66-25-1) analytical standards were purchased from Sigma Aldrich (Steinheim, Germany). Analytical grade chloroform, acetic acid (VWR Chemicals, Radnor, PA, USA), sodium thiosulfate, native potato starch (POCh, Gliwice, Poland), and potassium iodide were used in PV determination.

2.2. Experimental setup

In the described experiment three modifications of the experimental setup were used, namely for real-time analysis with PTR-MS, sampling for GC-FID, and sampling for GC-MS analysis. The scheme of the above-mentioned setups was placed in Fig. 1.

a. Real-time monitoring using PTR-MS (Fig. 1.a).

The experimental setup for measuring the composition of frying fumes using PTR-MS was described elsewhere in detail (Majchrzak & Wasik, 2021). Briefly, air from a cylinder at a continuous flow of 0.5 L/min was transferred through an air-tight glass reaction chamber where the glass beaker with oil was heated. The tuber cube stuck to the metal rod was immersed in the oil without opening the reaction chamber. The frying fumes were passed through the PTFE capillary and were split in the metal T-piece. The 0.1 L/min of fumes were transferred through the heated PEEK capillary to the PTR-MS device.

b. Tenax tube sampling for GC-FID analysis (Fig. 1.b).

For Tenax tube sampling the setup was modified by removing the PEEK capillary from one side of the T-piece and placing a glass tube packed with a 4 Å molecular sieve to remove moisture. Then the Tenax TA tube (Tenax TA stainless steel tubes, 35/60 mesh; Markes International Ltd.) was placed and the 200 mL of frying fumes were passed through the sorption medium. The analytes which occurs in fumes were collected just before frying started, after 5 min, and after 10 min of frying.

c. SPME sampling for GC-MS analysis.

Here, frying fumes were directly transferred (continuous flow of 0.5 L/min) to a 0.5 L Tedlar bag. Then, the SPME fiber was placed inside the Tedlar bag to extract the analytes. Samples were taken before frying started, after 1 min, and after 10 min of frying.

2.3. PTR-MS

The PTR TOF1000 ultra (Ionicon GmbH) operational parameters were described in detail in the previous work (Majchrzak & Wasik, 2021). The PTR-MS Viewer v3.4.3 (Ionicon GmbH) was used for data pre-processing. The E/N was set to 100 Td, and the diluted sample (100-times dilution using built-in dilution system) was transferred to the instrument. The drift tube temperature was kept at 70 °C. During the experiment, the water cluster ion signal (37.03 *m/z*; $H_5O_2^+$) was monitored and the signal remained unchanged throughout the analysis. The full, single MS spectrum was recorded each second of the measurement.

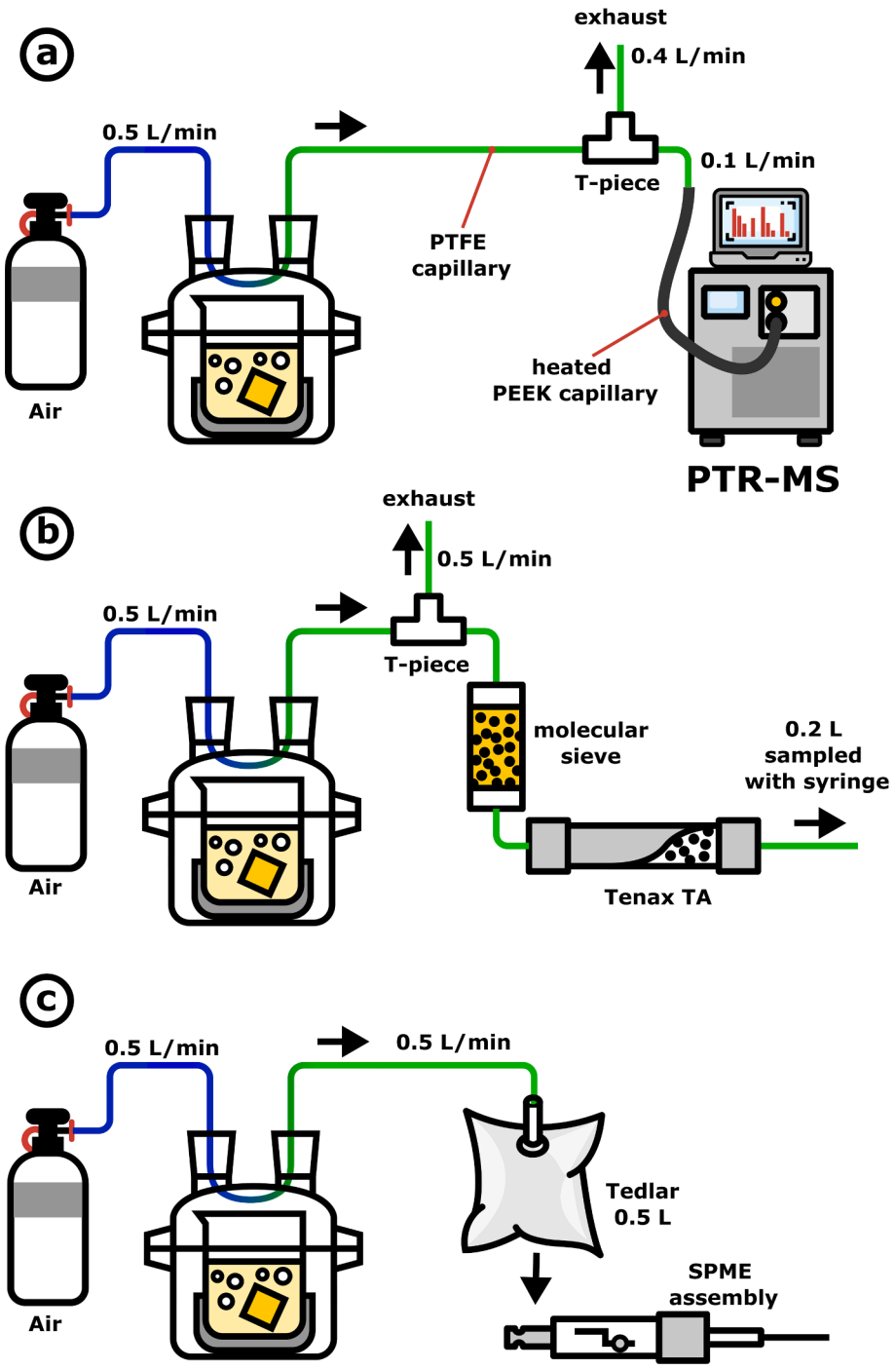

Fig. 1. Scheme of the experimental setup. The frying process took place in a closed reaction chamber and the frying fumes were transferred to PTR-MS for real-time monitoring (a); Tenax TA tube for targeted analysis using GC-FID (b); Tedlar bag for an omics-inspired approach based on GC-MS analysis (c).

2.4. TD-GC-FID

Analytes adsorbed on a Tenax TA were liberated using thermal desorption (TD) (Markes Series 2 Thermal Desorption Systems; UNITY/TD-100). Detailed information regarding this extraction technique and equipment specifications can be found in previous publications (Król, Zabiegała, & Namieśnik, 2012; Marć, Namieśnik, & Zabiegała, 2014; Marć & Zabiegała, 2017). In brief, samples (Tenax TA tubes) were heated to 285 °C for 12 min in a constant flow of helium at 50 mL/min. During this process, analytes were transferred to the microtrap (0 °C) sorption medium (Tenax TA and Carbotrap). Next, the analytes retained on the microtrap sorption bed were thermally extracted (ballistic heating) at 300 °C for 5 min and transported directly to the GC column in a constant flow of helium at 2 mL/min. The temperature of the transfer line between TD and GC was set to 180 °C. Separation and the quantitative analysis were performed using a GC-FID system (Agilent 7820A GC; Agilent Technologies, Inc.) under the conditions presented in Table 1. The GC capillary column (DB-1, Agilent Technologies, 123–1035) dimensions were 30 m × 320 μm × 5 μm. The FID working temperature was set to 280 °C and the constant gas flow rate through the GC column was set to 2 mL/min.

Table 1
Gas chromatography conditions for GC-FID and GC-MS analysis.

Analysis	Column	Flow rate	Initial temperature	Ramp 1	Hold temperature	Ramp 2	Final temperature	Total time
GC-FID	DB-1	2.0 mL/min	45.0 °C (1 min)	15.0 °C/min	120 °C (2 min)	10.0 °C/min	250 °C (5 min)	26.0 min
GC-MS	Equity-1	1.0 mL/min	40.0 °C (3 min)	3.0 °C/min	150 °C (3 min)	12.0 °C/min	250.0 °C (5 min)	56.0 min

2.5. SPME-GC-MS

The frying fumes components were extracted from the Tedlar bag using SPME fiber. Analytes collected in a Tedlar bag were extracted using the DVB/CAR/PDMS (2 cm, 50/30 μm, Supelco Inc., Bellefonte, USA) fiber for 30.0 min at room temperature. Afterwards, the fiber was transferred to the splitless injector and thermally desorbed for 4 min at 250 °C. The Agilent 7890A (Agilent Technologies, Santa Clara, USA) gas chromatograph coupled to Pegasus 4D TOFMS (LECO Corp., Saint Joseph, USA) was used. The separation of volatiles took place in the Equity 1 (30 m × 0.25 mm × 0.25 μm,) (Supelco Inc., Bellefonte, USA) column (for temperature programme see Table 1). The helium of high purity at a flow of 1.0 mL/min was used as the carrier gas. Both the transfer line and ion source temperature were set to 250 °C. The detector voltage was 1700 V and the ionisation energy was set to 70 eV. The spectra were acquired at the rate of 10 Hz with the ion mass range of 40–300 *m/z*. Raw CDF files were exported using Leco ChromaTOF 4.51.6.0 software and transferred for further processing.

2.6. Data analysis

The GC-MS raw data were pre-processed, which included chromatogram construction, noise subtraction, deconvolution, and data matrix alignment using the MZmine 2 software (Pluskal, Castillo, Villar-Briones, & Orešič, 2010). The resulting MZxml files were uploaded to the GNPS molecular networking software (Aksenov et al., 2021; M. Wang et al., 2016a, 2016b). The molecular network was generated and modified using Cytoscape v. 3.8.2. The tentative identification of compounds based on MS spectra was performed by comparison to the NIST Mass Spectral Library v. 2.0. The rest of the data were processed in Excel or using in-house Python algorithms.

3. Results and discussion

3.1. Targeted approach for real-time monitoring of volatiles during deep-frying using TD-GC-FID

The compounds of interest in this experiment were pentanal and hexanal. Those two aldehydes can be formed during the oxidation of n-6 PUFAs (Frankel, 1983). These compounds exhibit pulmonary toxicity and may affect, among others, sensory organ development, induction of apoptosis, reproductive developmental process (pentanal) and G-protein coupled receptor protein signalling pathway and pose acute inflammatory response (hexanal) (Cho, Song, Kim, & Ryu, 2018). First, the concentration of pentanal (Fig. 2.A) and hexanal (Fig. 2.B) in fumes emitted during deep-frying of *Gala* potato cube at 180 °C were determined using TD-GC-FID. Despite the controlled conditions, the concentration of volatiles in each run was significantly different; however, the general trend of increasing emission of pentanal and hexanal can be observed. The concentration of selected aldehydes in fumes of heated oil was 1.73 μg/L (in a range of 0.31 to 3.91 μg/L) and 0.61 μg/L (from 0.30 to 0.93 μg/L), for pentanal and hexanal respectively. After 10 min of frying their concentration in fumes increased to 6.70 μg/L (from 13.17 to 3.45 μg/L) for pentanal and 1.31 μg/L (from 1.95 to 0.67 μg/L) for hexanal. The concentration of pentanal is higher than hexanal which meets the agreement with other reported studies (Liu et al., 2020). Based on the TD-GC-FID analysis it can be considered that the emission of pentanal and hexanal has close-to-linear characteristics. However, real-time PTR-MS monitoring can verify this statement. In the first minute of frying, the bursting peak in the emission profile appeared. This rapid increase in aldehydes concentration could be related to the quick water evaporation

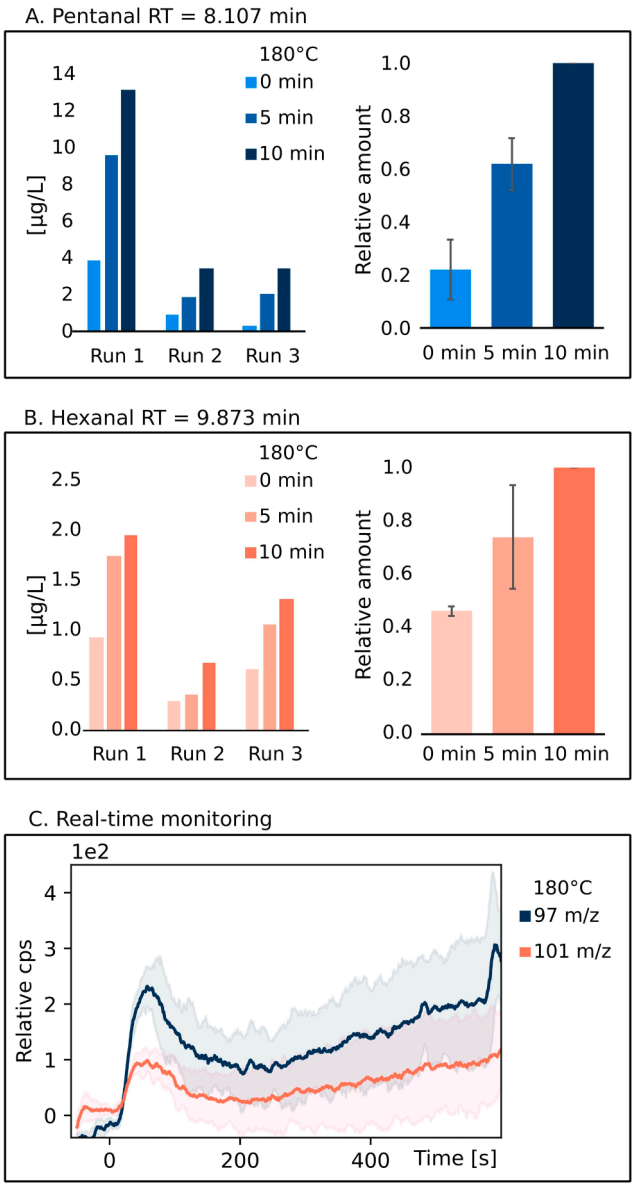

Fig. 2. Emission of pentanal and hexanal during deep-frying of a 5 g *Gala* potato cube in rapeseed oil at 180 °C; The concentration of pentanal (A) and hexanal (B) in the fumes just before frying (0 min) and after 5 and 10 min of frying. Quantification was performed in triplicate (runs) using a TD-GC-FID setup. Emission profiles (C) of pentanal (97 *m/z*) and hexanal (101 *m/z*) are shown as relative cps, where time 0 s is the moment of cube immersion. The signal was smoothed using a moving average (n = 10). Shaded areas represent standard deviations (n = 3). Real-time monitoring was obtained using a PTR-MS setup.

from the potato cube. Since lipid oxidation progresses during oil heating, the aldehydes can be formed and can be presented in the oil bulk. Then, right after immersion of the potato cube, the evaporated water formed gas bubbles and ejected this volatiles into the frying fumes. After a few minutes, when the water evaporation lowered and the crust formed, the amount of pentanal and hexanal drops down and the emission remained linear throughout the rest of frying.

A comparison of emission profiles for different frying scenarios is depicted in Fig. 3. It can be observed that the higher the frying temperature is, the higher the pentanal and hexanal emission is. At 140 °C (Fig. 3.A) the emission curve is almost flat, and the impact of the immersed potato cube is imperceptible. The increase of the frying temperature to 160 °C (Fig. 3.B) results in an increase in pentanal and hexanal concentration. Here, the bursting peak for pentanal in the first minutes of frying is also noticeable, however, is relatively smaller than for the oil heated to 180 °C (Fig. 3.C). This can be, for instance, related to the higher temperature and longer time to heat the oil to reach the final temperature. Both, heating time and temperature, are the well-known factors which catalyzed lipid oxidation (Choe & Min, 2007). It is possible to observe that using sweet potato (Fig. 3D) promotes the formation of pentanal. The bursting peaks of both compounds are much smaller than while frying *Gala* cube and the emission curve of pentanal flattened after approx. 7 min of frying. The smaller bursting peaks are also noticeable while frying of *Innovator* potato (Fig. 3.E). This could be related to lower water content in the *Innovator* than in the *Gala* cultivar. While increasing the size of the *Innovator* potato cube (3.0 ± 0.2 cm and weight of 10.0 ± 0.1 g) (Fig. 3.F) it is possible to observe the general increase of the recorded signal together with the higher bursting peak.

Based on the obtained results it can be stated that using PTR-MS to monitor the emission of pentanal and hexanal provides more comprehensive information about their appearance in frying fumes than using gas chromatography. Additionally, it should be pointed out that the first minutes of frying results in the intense emission of volatile compounds, thus in an omics-inspired approach the samples were taken before, and after 1 min and 10 min of frying.

3.2. Omics-inspired approach for real-time monitoring of volatiles during deep-frying using SPME-GC-MS

For the omic-inspired approach, the MN was performed based on SPME-GC-MS data and is shown in Fig. 4. The samples come from the experiment where fumes were emitted during the frying of the *Gala* potato at 180 °C. The domination of yellow-colored nodes suggests that the vast majority of volatiles were detected in the sample taken after 10 min of frying. There are only a few compounds that were present mostly before frying. An example could be 1,4-heptadiene (Fig. 3.B). A closer look at the nearest nodes connected to this compound in MN can lead to the conclusion that the emission of 1,4-heptadiene is becoming less intense over time of frying while the emission of oxygenated molecules starts to arise. Since the nodes are strongly connected, those compounds are possibly a product of the same process (1), came from the same substrate (2) or follow the same reaction chain (3). The compounds closely connected to the 1,4-heptadiene in MN are listed in Table S3 (Supplementary Materials).

The end-products in this network are 2-heptanone and octanal, both lipid oxidation products, and limonene. The 2-heptanone is both the major aroma compound (Zhang et al., 2021) and one of the rapeseed oil β-oxidation products (Gracka, Jeleń, Majcher, Siger, & Kaczmarek, 2016). Furthermore, it is known as a 13-hydroperoxy-10,12-cyclic peroxide decomposition product (Frankel, 1983). It is also reported that octanal can be formed in the haemolytic fission of the R–O bond of oleic acid, which occurs during the degradation of this fatty acid (Fullana, Carbonell-Barrachina, & Sidhu, 2004). It is also possible to find confirmation that limonene emits during the frying process (Chemat et al., 2004). The formation of limonene may be through cyclization reactions, which are common during oil degradation processes (Wang et al., 2016a, 2016b).

To confirm the relation between the emission of 1,4-heptadiene and 1-heptanone, octanal and limonene the real-time emission curves were plotted in Fig. 5. Data were present as cumulative curves to register the total amount of emitted compounds throughout 10 min of frying. The slope of the cumulative emission curve indicates the emission rate – the

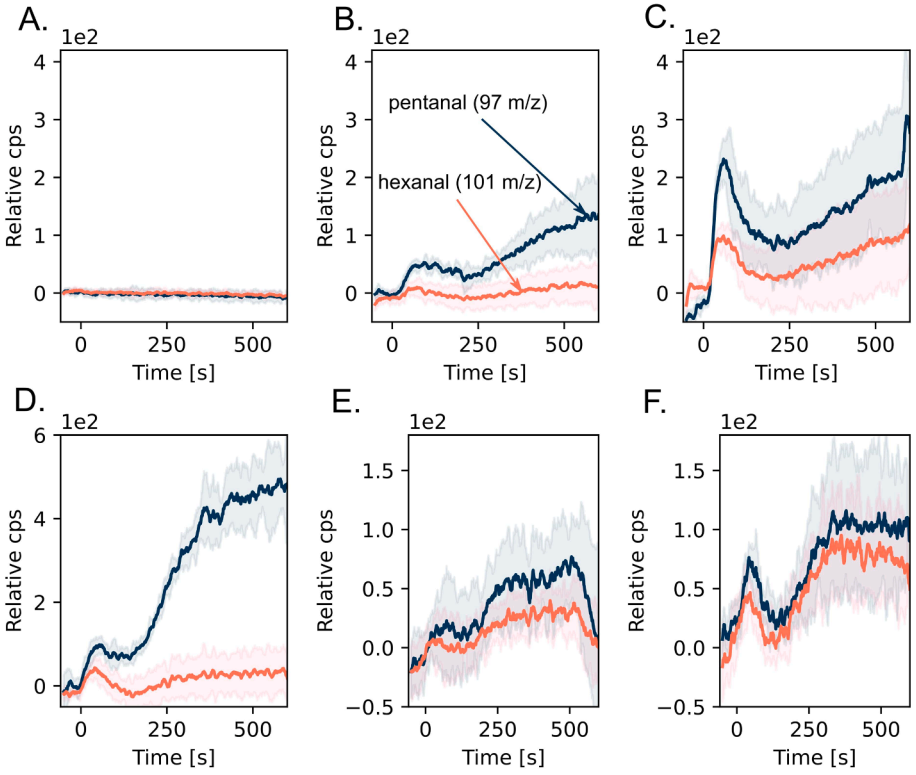

Fig. 3. Emission profiles of pentanal (97 *m/z*) and hexanal (101 *m/z*) are depicted as relative cps, where time 0 s is the moment of cube immersion. Here, six different frying scenarios were presented: A- frying temperature of 140 °C, *Gala* potato, 5 g cube; B- 160 °C, *Gala* potato, 5 g cube; C- 180 °C, *Gala* potato, 5 g cube; D- 180 °C, sweet potato, 5 g cube; E- 180 °C, *Innovator* potato, 5 g cube; G- 180 °C, *Innovator* potato, 10 g cube. The signal was smoothed using a moving average (n = 10). Shaded areas represent standard deviations (n = 3).

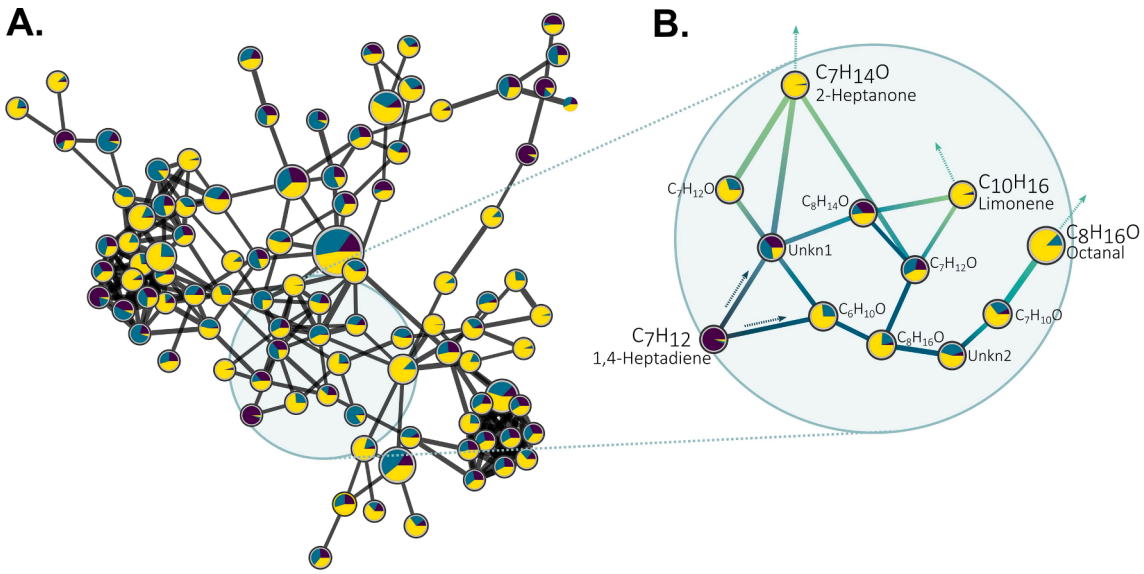

Fig. 4. The result of molecular networking (MN) represents the correlation of the volatiles emitted in the frying fumes during deep-frying at 180 °C just before frying (0 min) and after 1 and 10 min of frying. The nodes represent the individual volatile compounds and edges were formed according to cosine similarity (CS greater than 0.75). Edge thickness represents the CS – the thicker the edge, the higher the CS (A). The node size is related to the peak area. The pie charts depict peak area distribution in 0 min sample (dark blue), 1 min (teal), and 10 min (yellow). The general view of MN is shown in A; the zoom-in of 1,4-heptadiene MN is shown in B. (For interpretation of the references to colour in this figure legend, the reader is referred to the web version of this article.)

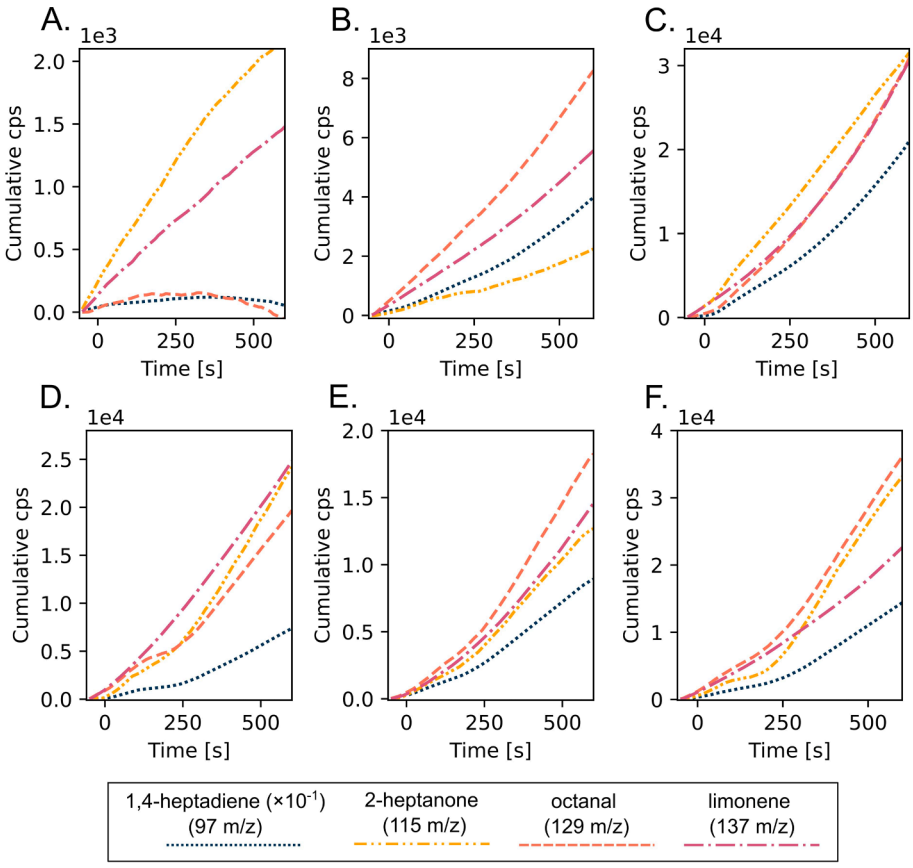

Fig. 5. The emission profiles of 1,4-heptadiene (97 *m/z*) 2-heptanone (115 *m/z*), limonene (137 *m/z*), and octanal (129 *m/z*) for six different frying scenarios: A- frying at 140 °C, *Gala* potato, 5 g cube; B- 160 °C, *Gala* potato, 5 g cube; C- 180 °C, *Gala* potato, 5 g cube; D- 180 °C, sweet potato, 5 g cube; F- 180 °C, Innovator potato, 5 g cube; G- 180 °C, *Innovator* potato, 10 g cube. Emission profiles are shown as cumulative, relative cps, where zero is time 0 s (the moment of cube immersion). The signal was smoothed using a moving average (n = 10).

steeper the slope is the emission of volatiles is more intense. As can be seen in Fig. 5 the most abundant compound of the four selected is 1,4-heptadiene. For the sake of clarity in Fig. 5 the registered cumulative cps were lowered 10-times for this compound. It can be also observed that after approx. 5 min of frying the emission curve for 1,4-heptadiene has become steeper. This, in turn, could undermine the results obtained from MN experiment, where the 1,4-heptadiene is almost not present in the samples taken after one minute and 10 min after the cube was immersed. Supposedly, in the presence of a high load of volatiles, there is competition for the absorption sites in the SPME fiber, resulting in

smaller peak area of 1,4-heptadiene.

The highest cumulative emission of 1,4-heptadiene can be recorded in fumes while frying *Gala* cultivar at 180 °C. Although, for most of the registered scenarios (Fig. 5.B-F) the emission curve of this compound exhibits a similar shape. The exception is frying at the lowest tested temperature, in 140 °C, where the emission curve is almost flat (Fig. 5. A). In this temperature of frying a similar characteristic can be plotted for octanal, whereas limonene and 2-heptanone curves increase. Considering the emission of those three volatile products, it is possible to observe the temperature-related emission, which becomes the highest when the frying is taken place at 180 °C (Fig. 5. A-C). Most of the cumulative curves fit accurately the quadratic equation, which was also demonstrated in the previous studies (Majchrzak & Wasik, 2021; Wichrowska & Majchrzak, 2021).

In plots Fig. 5. D-E the emission profile resulted from the frying experiments where the sweet potato and *Innovator* cultivar were fried. Compared to the *Gala* cultivar, the cumulative emission was significantly lower when the *Innovator* cultivar and sweet potato were fried. This might be due to the lower water content; however, this relation is not evident. In the frying scenario with the sweet potato, the emission of all of the plotted ions rises in a close-to-linear manner in the first minute of frying and after that time 2-heptanone and octanal emissions diminish and continue growing after 5 min. The 137 *m/z* ion (limonene) is the most abundant ion in this scenario. In the case of using *Innovator* for frying, the highest registered compound octanal.

The last plot (Fig. 5. F) depicts the situation where an *Innovator* cultivar potato cube of double size was immersed in rapeseed oil heated to 180 °C. This resulted in a slightly higher emission of all plotted volatiles; however, the effect of a larger cube was not as significant as the type of tuber placed in the oil. This higher emission can be related to the larger surface area as well as the larger water volume. The shape of the cumulative emission curve is also different, which suggests that the cube size also affects the emission characteristic of particular compounds.

Those VOCs are also associated with possible inhalation health risks. The hexanal and octanal have been proven to pose a potential carcinogenic risk (margin of exposure - MOE < 1) (Zhang, Liu, Jia, Wang, & Han, 2019). The presence of aldehydes in the inhaled air may also affect the development of respiratory diseases such as asthma and COPD. Octanal can induce lung damage (Song et al., 2014) including modifying the miRNA expression (Song et al., 2014). On the other hand, limonene, like most monoterpenes, is responsible for SOA formation (Murugachandran, Tang, Peña, Loru, & Sanz, 2021; Spittler et al., 2006), which may contribute to the deterioration of indoor air quality. SOAs have also been shown to be present in cooking fumes (Zhu et al., 2021).

4. Conclusions

Real-time tracking of the emission of volatile thermal degradation products can provide valuable information on the transformations that occur in the first minutes of frying. For example, a sudden outburst of volatile products, such as aldehydes, can be recorded. However, this finding could have been overlooked if a more standard approach, such as a GC, had been used. Due to the versatility of the proposed solution, in which PTR-MS is the centrepiece, it was possible to develop two measurement approaches. In the first, targeted approach it was possible to quantify the pentanal and hexanal using TD-GC-FID. The obtained results suggested that the emission of those aldehydes is close to linear, whereas during PTR-MS real-time measurements it was proven to register high outburst of those aldehydes in the first minutes of frying. In the second, the MN based on SPME-GC-MS data were performed to find characteristic correlations between emitted volatiles. Based on obtained results from this experiment it was possible to suggest that, the emitted before frying, 1,4-heptadiene was transferred to 2-heptanone, octanal and limonene during the deep-frying process. However, it was revalidated using PTR-MS and the 1,4-heptadiene was emitted throughout the whole experiment. In the case of both approaches, the different frying temperatures, different tuber types and cube sizes were tested to observe differences in emission profile.

The proposed approaches may also find application in tracking transformations during various food preparation processes as well as in industrial or environmental emission studies. Detailed understanding of the processes occurring during the dynamic frying process, part of which involves the study of the profiling of the emission of volatiles, can be a valuable tool in food engineering. Moreover, it may lead to the development of solutions reducing the emission of, often harmful, compounds to indoor air inside kitchens or food processing plants.

CRediT authorship contribution statement

Tomasz Majchrzak: Conceptualization, Methodology, Validation, Formal analysis, Investigation, Visualization, Funding acquisition, Writing - original draft, Writing - review & editing. **Mariusz Marć:** Methodology, Formal analysis, Investigation, Writing - review & editing. **Andrzej Wasik:** Writing – review & editing, Supervision.

Declaration of Competing Interest

The authors declare that they have no known competing financial interests or personal relationships that could have appeared to influence the work reported in this paper.

Acknowledgments

This research was funded by the National Science Centre, Poland, grant number 2018/31/N/NZ9/02404.

Data Availability Statement

The data presented in this study are available on request from the corresponding author. The whole GNPS pipeline and raw data are available in the MassIVE online repository from the GNPS (https://gnps.ucsd.edu/ProteoSAFe/status.jsp?task=8964997a72734fae849c8046379ebf79).

Appendix A. Supplementary material

Supplementary data to this article can be found online at https://doi.org/10.1016/j.foodres.2022.111716.

References

Aksenov, A. A., Laponogov, I., Zhang, Z., Doran, S. L. F., Belluomo, I., Veselkov, D., … Veselkov, K. (2021). Auto-deconvolution and molecular networking of gas chromatography–mass spectrometry data. *Nature Biotechnology, 39*(2), 169–173. https://doi.org/10.1038/s41587-020-0700-3

Arata, C., Misztal, P. K., Tian, Y., Lunderberg, D. M., Kristensen, K., Novoselac, A., Vance, M. E., Farmer, D. K., Nazaroff, W. W., & Goldstein, A. H. (2021). Volatile organic compound emissions during HOMEChem. *Indoor Air, 31*(6), 2099–2117. https://doi.org/10.1111/INA.12906

Arı, A., Ertürk Arı, P., Yenïsoy-Karakaş, S., & Gaga, E. O. (2020). Source characterization and risk assessment of occupational exposure to volatile organic compounds (VOCs) in a barbecue restaurant. *Building and Environment, 174*, 106791. https://doi.org/10.1016/j.buildenv.2020.106791

Atamaleki, A., Motesaddi Zarandi, S., Massoudinejad, M., Esrafili, A., & Mousavi Khaneghah, A. (2022). Emission of BTEX compounds from the frying process: Quantification, environmental effects, and probabilistic health risk assessment. *Environmental Research, 204*, 112295. https://doi.org/10.1016/J.ENVRES.2021.112295

Biasioli, F., Gasperi, F., Yeretzian, C., & Märk, T. D. (2011). PTR-MS monitoring of VOCs and BVOCs in food science and technology. *TrAC - Trends in Analytical Chemistry, 30*(7), 968–977. https://doi.org/10.1016/j.trac.2011.03.009

Bordin, K., Kunitake, M. T., Aracava, K. K., & Trindade, C. S. F. (2013). Changes in food caused by deep fat frying - A review. *Archivos Latinoamericanos de Nutricion*. https://www.alanrevista.org/ediciones/2013/1/art-1/.

Bouchon, P. (2009). Understanding Oil Absorption During Deep-Fat Frying. In *Advances in Food and Nutrition Research* (1st ed., Vol. 57, Issue 09). Elsevier Inc. https://doi.org/10.1016/S1043-4526(09)57005-2.

Chemat, F., Grondin, I., Costes, P., Moutoussamy, L., Sing, A. S. C., & Smadja, J. (2004). High power ultrasound effects on lipid oxidation of refined sunflower oil. *Ultrasonics Sonochemistry, 11*(5), 281–285. https://doi.org/10.1016/j.ultsonch.2003.07.004

Cho, Y., Song, M. K., Kim, T. S., & Ryu, J. C. (2018). DNA methylome analysis of saturated aliphatic aldehydes in pulmonary toxicity. *Scientific Reports, 8*(1), 1–10. https://doi.org/10.1038/s41598-018-28813-z

Choe, E., & Min, D. B. (2007). Chemistry of deep-fat frying oils. *Journal of Food Science, 72*(5), 1–10. https://doi.org/10.1111/j.1750-3841.2007.00352.x

Dimitri, G., van Ruth, S. M., Sacchetti, G., Piva, A., Alewijn, M., & Arfelli, G. (2013). PTR-MS monitoring of volatiles fingerprint evolution during grape must cooking. *LWT - Food Science and Technology, 51*(1), 356–360. https://doi.org/10.1016/j.lwt.2012.10.004

Ellis, A. M., & Mayhew, C. A. (2014). Proton Transfer Reaction Mass Spectrometry. In *Proton Transfer Reaction Mass Spectrometry: Principles and Applications*. https://doi.org/10.1002/9781118682883.

Frankel, E. N. (1983). Volatile lipid oxidation products. *Progress in Lipid Research, 22*(1), 1–33. https://doi.org/10.1016/0163-7827(83)90002-4

Fullana, A., Carbonell-Barrachina, Á. A., & Sidhu, S. (2004). Volatile aldehyde emissions from heated cooking oils. *Journal of the Science of Food and Agriculture, 84*(15), 2015–2021. https://doi.org/10.1002/jsfa.1904

Gloess, A. N., Vietri, A., Wieland, F., Smrke, S., Schönbächler, B., López, J. A. S., Petrozzi, S., Bongers, S., Koziorowski, T., & Yeretzian, C. (2014). Evidence of different flavour formation dynamics by roasting coffee from different origins: On-line analysis with PTR-ToF-MS. *International Journal of Mass Spectrometry, 365–366*, 324–337. https://doi.org/10.1016/j.ijms.2014.02.010

Gracka, A., Jeleń, H. H., Majcher, M., Siger, A., & Kaczmarek, A. (2016). Flavoromics approach in monitoring changes in volatile compounds of virgin rapeseed oil caused by seed roasting. *Journal of Chromatography A, 1428*, 292–304. https://doi.org/10.1016/j.chroma.2015.10.088

Hansel, A., Jordan, A., Holzinger, R., Prazeller, P., Vogel, W., & Lindinger, W. (1995). Proton transfer reaction mass spectrometry: On-line trace gas analysis at the ppb level. *International Journal of Mass Spectrometry and Ion Processes, 149–150*(C), 609–619. https://doi.org/10.1016/0168-1176(95)04294-U

Hewitt, C. N., Hayward, S., & Tani, A. (2003). The application of proton transfer reaction-mass spectrometry (PTR-MS) to the monitoring and analysis of volatile organic compounds in the atmosphere. *Journal of Environmental Monitoring, 5*(1), 1–7. https://doi.org/10.1039/b204712h

Hosseini, H., Ghorbani, M., Meshginfar, N., & Mahoonak, A. S. (2016). A Review on Frying: Procedure, Fat, Deterioration Progress and Health Hazards. *JAOCS, Journal of the American Oil Chemists' Society, 93*(4), 445–466. https://doi.org/10.1007/s11746-016-2791-z

Katragadda, H. R., Fullana, A., Sidhu, S., & Carbonell-Barrachina, Á. A. (2010). Emissions of volatile aldehydes from heated cooking oils. *Food Chemistry, 120*(1), 59–65. https://doi.org/10.1016/j.foodchem.2009.09.070

Król, S., Zabiegała, B., & Namieśnik, J. (2012). Measurement of benzene concentration in urban air using passive sampling. *Analytical and Bioanalytical Chemistry, 403*(4), 1067–1082. https://doi.org/10.1007/s00216-011-5578-y

Liu, Z. Y., Zhou, D. Y., Li, A., Zhao, M. T., Hu, Y. Y., Li, D. Y., Xie, H. K., Zhao, Q., Hu, X. P., Zhang, J. H., & Shahidi, F. (2020). Effects of temperature and heating time on the formation of aldehydes during the frying process of clam assessed by an HPLC-MS/MS method. *Food Chemistry, 308*, 125650. https://doi.org/10.1016/j.foodchem.2019.125650

López, J. A. S., Wellinger, M., Gloess, A. N., Zimmermann, R., & Yeretzian, C. (2016). Extraction kinetics of coffee aroma compounds using a semi-automatic machine: On-line analysis by PTR-ToF-MS. *International Journal of Mass Spectrometry, 401*, 22–30. https://doi.org/10.1016/j.ijms.2016.02.015

Lu, F., Shen, B., Li, S., Liu, L., Zhao, P., & Si, M. (2021). Exposure characteristics and risk assessment of VOCs from Chinese residential cooking. *Journal of Environmental Management, 289*, 112535. https://doi.org/10.1016/j.jenvman.2021.112535

Majchrzak, T., & Wasik, A. (2021). Release Kinetics Studies of Early-Stage Volatile Secondary Oxidation Products of Rapeseed Oil Emitted during the Deep-Frying Process. *Molecules (Basel, Switzerland), 26*(4), 1006. https://doi.org/10.3390/molecules26041006

Majchrzak, T., Wojnowski, W., Głowacz-Różyńska, A., & Wasik, A. (2021). On-line assessment of oil quality during deep frying using an electronic nose and proton transfer reaction mass spectrometry. Food Control, 121, 107659. https://doi.org/10.1016/j.foodcont.2020.107659.

Majchrzak, T., Wojnowski, W., Lubinska-Szczygeł, M., Różańska, A., Namieśnik, J., & Dymerski, T. (2018). PTR-MS and GC-MS as complementary techniques for analysis of volatiles: A tutorial review. *Analytica Chimica Acta*. https://doi.org/10.1016/j.aca.2018.06.056

Majchrzak, T., Wojnowski, W., Rutkowska, M., & Wasik, A. (2020). Real-Time Volatilomics: A Novel Approach for Analyzing Biological Samples. In *Trends in Plant Science* (Vol. 25(3), pp. 302–312). Elsevier Ltd.. https://doi.org/10.1016/j.tplants.2019.12.005

Majchrzak, T., Wojnowski, W., & Wasik, A. (2021b). Revealing dynamic changes of the volatile profile of food samples using PTR–MS. *Food Chemistry, 364*, 130404. https://doi.org/10.1016/j.foodchem.2021.130404

Marć, M., Namieśnik, J., & Zabiegała, B. (2014). Small-scale passive emission chamber for screening studies on monoterpene emission flux from the surface of wood-based indoor elements. *Science of the Total Environment, 481*(1), 35–46. https://doi.org/10.1016/j.scitotenv.2014.02.021

Marć, M., & Zabiegała, B. (2017). An investigation of selected monoaromatic hydrocarbons released from the surface of polystyrene lids used in coffee-to-go cups. *Microchemical Journal, 133*, 496–505. https://doi.org/10.1016/j.microc.2017.04.015

Mogol, B. A., & Gökmen, V. (2016). Thermal process contaminants: Acrylamide, chloropropanols and furan. In *Current Opinion in Food Science* (Vol. 7, pp. 86–92). https://doi.org/10.1016/j.cofs.2016.01.005.

Murugachandran, S. I., Tang, J., Peña, I., Loru, D., & Sanz, M. E. (2021). New Insights into Secondary Organic Aerosol Formation: Water Binding to Limonene. *Journal of Physical Chemistry Letters, 12*(3), 1081–1086. https://doi.org/10.1021/acs.jpclett.0c03574

Pico, J., Khomenko, I., Capozzi, V., Navarini, L., & Biasioli, F. (2020). Real-time monitoring of volatile compounds losses in the oven during baking and toasting of gluten-free bread doughs: A PTR-MS evidence. *Foods, 9*(10), 1498. https://doi.org/10.3390/foods9101498

Pluskal, T., Castillo, S., Villar-Briones, A., & Orešič, M. (2010). MZmine 2: Modular framework for processing, visualizing, and analyzing mass spectrometry-based molecular profile data. *BMC Bioinformatics, 11*(1), 1–11. https://doi.org/10.1186/1471-2105-11-395

Schneider, M. V., & Orchard, S. (2011). Omics technologies, data and bioinformatics principles. *Methods in Molecular Biology (Clifton N.J.), 719*, 3–30. https://doi.org/10.1007/978-1-61779-027-0_1

Song, M. K., Choi, H. S., Lee, H. S., Kim, Y. J., Park, Y. K., & Ryu, J. C. (2014). Analysis of microRNA and mRNA expression profiles highlights alterations in modulation of the MAPK pathway under octanal exposure. *Environmental Toxicology and Pharmacology, 37*(1), 84–94. https://doi.org/10.1016/j.etap.2013.11.005

Song, M. K., Lee, H. S., Choi, H. S., Shin, C. Y., Kim, Y. J., Park, Y. K., & Ryu, J. C. (2014). Octanal-induced inflammatory responses in cells relevant for lung toxicity: Expression and release of cytokines in A549 human alveolar cells. *Human and Experimental Toxicology, 33*(7), 710–721. https://doi.org/10.1177/0960327113506722

Spittler, M., Barnes, I., Bejan, I., Brockmann, K. J., Benter, T., & Wirtz, K. (2006). Reactions of NO3 radicals with limonene and α-pinene: Product and SOA formation. *Atmospheric Environment, 40*, 116–127. https://doi.org/10.1016/j.atmosenv.2005.09.093

Stevens, J. F., & Maier, C. S. (2008). Acrolein: Sources, metabolism, and biomolecular interactions relevant to human health and disease. *Molecular Nutrition and Food Research, 52*(1), 7–25. https://doi.org/10.1002/mnfr.200700412

Vincenti, F., Montesano, C., Di Ottavio, F., Gregori, A., Compagnone, D., Sergi, M., & Dorrestein, P. (2020). Molecular Networking: A Useful Tool for the Identification of New Psychoactive Substances in Seizures by LC–HRMS. *Frontiers in Chemistry, 8*, 1039. https://doi.org/10.3389/FCHEM.2020.572952/BIBTEX

Wang, L., Csallany, A. S., Kerr, B. J., Shurson, G. C., & Chen, C. (2016). Kinetics of Forming Aldehydes in Frying Oils and Their Distribution in French Fries Revealed by LC-MS-Based Chemometrics. *Journal of Agricultural and Food Chemistry, 64*(19), 3881–3889. https://doi.org/10.1021/acs.jafc.6b01127

Wang, M., Carver, J. J., Phelan, V. V., Sanchez, L. M., Garg, N., Peng, Y., Nguyen, D. D., Watrous, J., Kapono, C. A., Luzzatto-Knaan, T., Porto, C., Bouslimani, A., Melnik, A. V., Meehan, M. J., Liu, W. T., Crüsemann, M., Boudreau, P. D., Esquenazi, E., Sandoval-Calderón, M., … Bandeira, N. (2016). Sharing and community curation of mass spectrometry data with Global Natural Products Social Molecular Networking. In *Nature Biotechnology* (Vol. 34, Issue 8, pp. 828–837). Nature Publishing Group. https://doi.org/10.1038/nbt.3597.

Wichrowska, W., & Majchrzak, T. (2021). Monitoring of Acrolein, Acetaldehyde and 1,3-Butadiene in Fumes Emitted during Deep-Frying of Potato Pieces in Rapeseed Oil Using PTR-MS. In *Dynamic Flavor: Capturing Aroma Using Real-Time Mass Spectrometry* (ACS Sympos, pp. 139–150). American Chemical Society.

Yao, Z., Li, J., Wu, B., Hao, X., Yin, Y., & Jiang, X. (2015). Characteristics of PAHs from deep-frying and frying cooking fumes. *Environmental Science and Pollution Research, 22*(20), 16110–16120. https://doi.org/10.1007/s11356-015-4837-4

Zhan, X., Duan, J., & Duan, Y. (2013). Recent developments of proton-transfer reaction mass spectrometry (PTR-MS) and its applications in medical research. *Mass Spectrometry Reviews, 32*(2), 143–165. https://doi.org/10.1002/mas.21357

Zhang, D. C., Liu, J. J., Jia, L. Z., Wang, P., & Han, X. (2019). Speciation of VOCs in the cooking fumes from five edible oils and their corresponding health risk assessments. *Atmospheric Environment, 211*, 6–17. https://doi.org/10.1016/j.atmosenv.2019.04.043

Zhang, Q., Saleh, A. S. M., Chen, J., & Shen, Q. (2012). Chemical alterations taken place during deep-fat frying based on certain reaction products: A review. *Chemistry and Physics of Lipids, 165*(6), 662–681. https://doi.org/10.1016/j.chemphyslip.2012.07.002

Zhang, Y., Wu, Y., Chen, S., Yang, B., Zhang, H., Wang, X., Granvogl, M., & Jin, Q. (2021). Flavor of rapeseed oil: An overview of odorants, analytical techniques, and impact of treatment. *Comprehensive Reviews in Food Science and Food Safety, 20*(4), 3983–4018. https://doi.org/10.1111/1541-4337.12780

Zhu, W., Guo, S., Zhang, Z., Wang, H., Yu, Y., Chen, Z., … Prévôt, A. S. H. (2021). Mass spectral characterization of secondary organic aerosol from urban cooking and vehicular sources. *Atmos. Chem. Phys, 21*, 15065–15079. https://doi.org/10.5194/acp-21-15065-2021